Tomography-based 3D Print Models of Sea Ice Microstructure

1 Introduction

Sea ice plays an important role in the climate system as sea ice insulates the ocean from the atmosphere. Exchange processes between the ocean and the atmosphere are controlled by the permeability of the sea ice. Hence, it is important to gain a good knowledge about the permeability. The microstructure and permeability of sea ice can be investigated non-destructively by means of microtomography.

During the eight weeks at the Geophysical Institute of the University Bergen, microtomographic images of sea ice samples were prepared for deriving the permeability of the sea ice samples. Both hydrodynamic simulations and laboratory experiments were conducted. For the laboratory experiments magnified 3D print models of the sea-ice samples were produced.

The sea-ice samples were collected both in the field and in the laboratory. First-year ice samples were taken in Svalbard fjords in spring 2009. The laboratory sea-ice samples were grown in 'The Kings Bay Marine Laboratory' in Ny Ålesund. The brine was centrifuged out of the sea-ice samples at the in-situ temperature to preserve the microstructure of the ice. Thus, only the pure ice lattice of the samples was left, which were stored at -80°C after centrifugation. The ice samples were then brought to the Institute for Snow and Avalanche Research (SLF) of the Swiss Federal Institute for Forest, Snow and Landscape Research (WSL) in Davos, where microtomographic images were taken of the samples in a computer tomograph. The samples had a diameter of 2cm. The voxel length of the images was 11.2µm and stacks of 366 images were created with the computer tomograph.

2 Preparation of the microtomographic images

The microtomographic images of the sea-ice samples (Figure 2.1 (a)) had to be further processed for the hydrodynamic simulations and the 3D prints. At first, a quadratic cutout of the image stack was done for the hydrodynamic simulations (Figure 2.1 (b)). With the program 'Image J' the greyscale images were transformed into binary images by segmentation (Figure 2.1 (c)). Therefore, a threshold for the differentiation between air (empty brine inclusions) and ice was used. For the 3D prints a circle cutout of the image stack was taken (Figure 2.1 (d)).

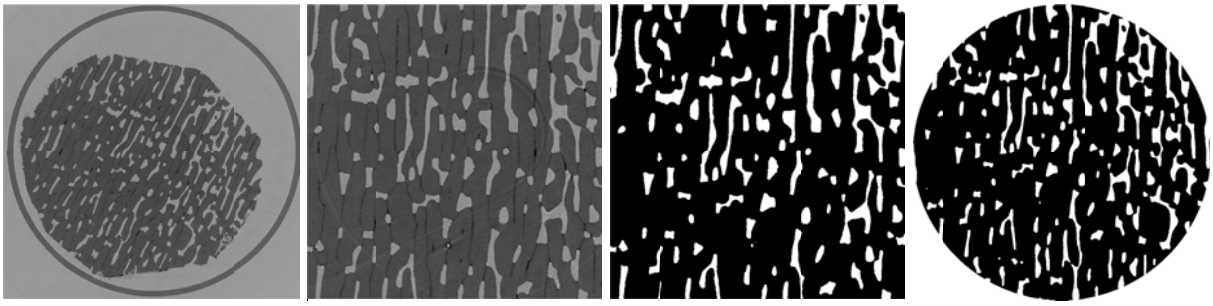

Figure 2.1: *Microtomographic image of a first-year ice sample (a), a quadratic cutout of the image for the hydrodynamic simulations (b), the segmentation in the quadratic cutout (c) and a circle cutout for the 3D print (d). In (a) and (b) the dark grey areas correspond to ice, the light grey areas to air and the small black areas to salt.*

3 Hydrodynamic simulations

The quadratic cutout of the segmented microtomographic image stack of the sea-ice samples (Figure 2.1 (c)) is taken to conduct hydrodynamic simulations with the program 'GeoDict' in order to determine the permeability in the vertical direction of the sample. In these virtual flow experiments a Newtonian fluid (in this case water at 0°C) flows through the sample. The permeability of the sample is calculated from Darcy's law:

$$Q = \frac{-kA}{\mu}\frac{(P_b - P_a)}{L}$$

Q corresponds to the total discharge in m^3/s, k to the permeability of the sample in m^2, A to the cross-sectional area of the sample in m^2, *(Pb-Pa)* to the pressure drop, μ to the viscosity of the water in Pa/s, and L corresponds to the length of the sample in m (Wiegmann (2012)). Darcy's law is only valid for very slow flows with a Reynoldsnumber less than 1, that follow the Stokes equation. This means that the relation between pressure drop and the flow velocity is linear. Therefore, the permeability can only be calculated for samples with small pore diameters since the flow through the pores has to be laminar. For the calculation of the permeability several equations for pressure and velocity values are solved iteratively at each voxel. The stopping criterion for the calculation is the stationarity of the process, which means a relative improvement in the permeability smaller than the chosen accuracy from one iteration to the next one. Additionally, a value for maximal iterations and the maximal run time is chosen, at which the calculation of the permeability stops, even though stationarity might not be reached yet. In addition to the permeability, some microstructural quantities of the sample, such as the pore size distribution and the porosity, are derived with GeoDict.

The results of the hydrodynamic simulations with GeoDict can not be presented in this report, since they are not finished yet. The permeability calculation for one sea-ice sample can last several days.

4 3D print models of sea ice

An 'UP! Plus 3D printer' was used to print the 3D sea-ice models (Figure 4.1 (a)). It is possible to print 14x14x13.5cm³ large objects with this printer, which is in the range of the sizes planned to print. The printer builds up a 3D object in 0.2mm thick layers of plastic. Therefore, a 1.75mm thick ABS (Acrylonitrile butadiene styrene) filament is melted at 260°C and given through a nozzle onto a heated perfboard, which is fixed with screws on the printer platform (Figure 4.1 (c)). Since the melted plastic is pushed into the perforations, the printed object is better fixed to the printer platform and does not lift easily. Moreover, a preheating of the perfboard for 15 minutes before printing also prevents the object to lift from the platform. Besides the 3D object itself, base and support material is printed. The base layers are first printed onto the perfboard (Figure 4.2 (b)) for an easier detachment of the 3D object from the perfboard after printing. Support material is printed for stabilization as a first layer onto the base layers before printing the 3D object (Figure 4.2 (c)). Moreover, support material is printed underneath overhanging parts of the 3D object and inside the object. The interior of the 3D object is never completely filled with plastic, but with a scaffold structure. In a very hollow structure support material can be printed inside the 3D object to strengthen the surface and bottom of the object. The outer wall thickness of the printed 3D object is 1.5mm.

The 3D printer can only print so-called stl-files ('StereoLithography'), in which the surface of the 3D object is represented by many triangular surfaces. These stl-files are loaded into the printer program, where they can be scaled and placed at the right position on the printer platform

(Figure 4.1 (b)). Moreover, the program indicates, whether the triangular surfaces are correctly orientated, which means that their normal has to face outwards. Wrong orientated surfaces are fixed with the program 'Netfabb Studio Professional' before loading the file into the printer program.

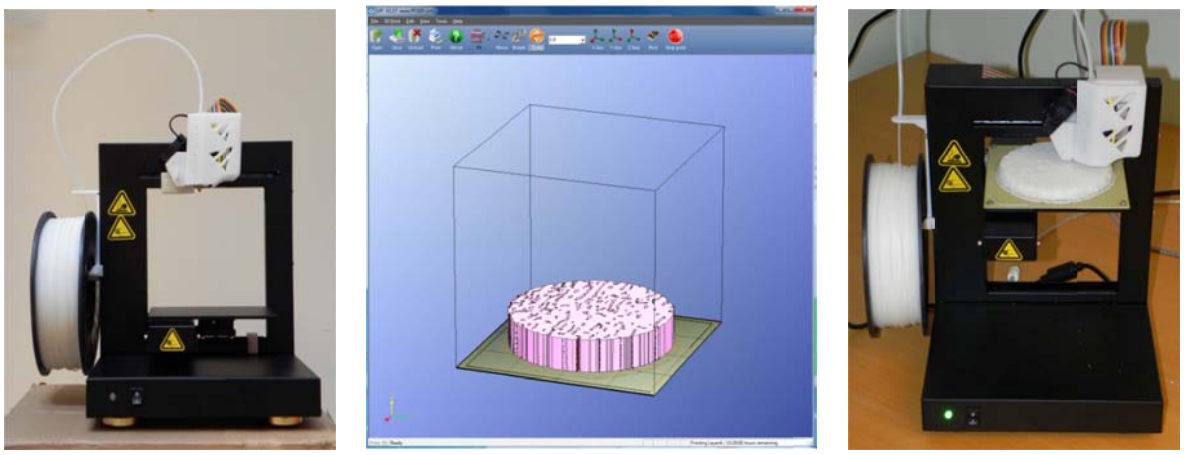

(a) (b) (c)

Figure 4.1: *The 'UP! Plus 3D printer' (a), printing of a sea-ice 3D print model (c) and the printer program with a loaded stl-file (b).*

Before printing the sea-ice models, a calibration print had to be done for a calibration of the printer (Figure 4.2). For the calibration the distances between the components on the edges of the print and the deviation of the 'L' shaped component (Figure 4.2 (c)) were measured.

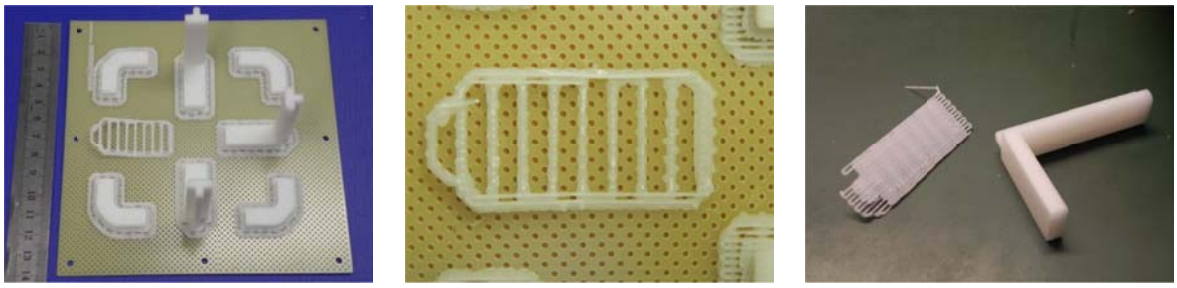

(a) (b) (c)

Figure 4.2: *Calibration print (a), the base layers of an 'L' shaped component of the calibration print (b) and the support material (c, left) of that component (c, right).*

Afterwards some test prints were made (Figure 4.3) in order to test the printer and to find out the best printer setup for the sea-ice print models. The test prints consisted of one stl-file from the internet (Figure 4.3 (a)), and three files that were created with GeoDict. With the module 'GridGeo' in GeoDict two idealized sea-ice samples with different heights and pore sizes were constructed (Figure 4.3 (b) and (c)). The third file was created from a microtomographic sea-ice image, which was repeated 30 times in order to get a thin 3D print (Figure 4.3 (d)). The test prints show that pore sizes of 2mm are possible to print. Furthermore, the test prints show how the properties of the base and support material and the 3D print model itself should be chosen. A 2mm thick base layer is sufficient for an easy removal of the finished print model from the

perfboard. Support material is printed underneath overhanging material with an angle less than a chosen value and with an area larger than a chosen value. In order to avoid support material to be printed into the pores of the sea-ice print models, the smallest angle possible (10°) and the largest area possible (20mm²) is chosen. Inside the sea-ice print models the smallest scaffold structure is chosen. Thus, there are as few openings as possible besides the pores, where a liquid could intrude into the model during the permeability experiments in the laboratory, in the case that the surface and walls of the 3D print model might not be closely printed.

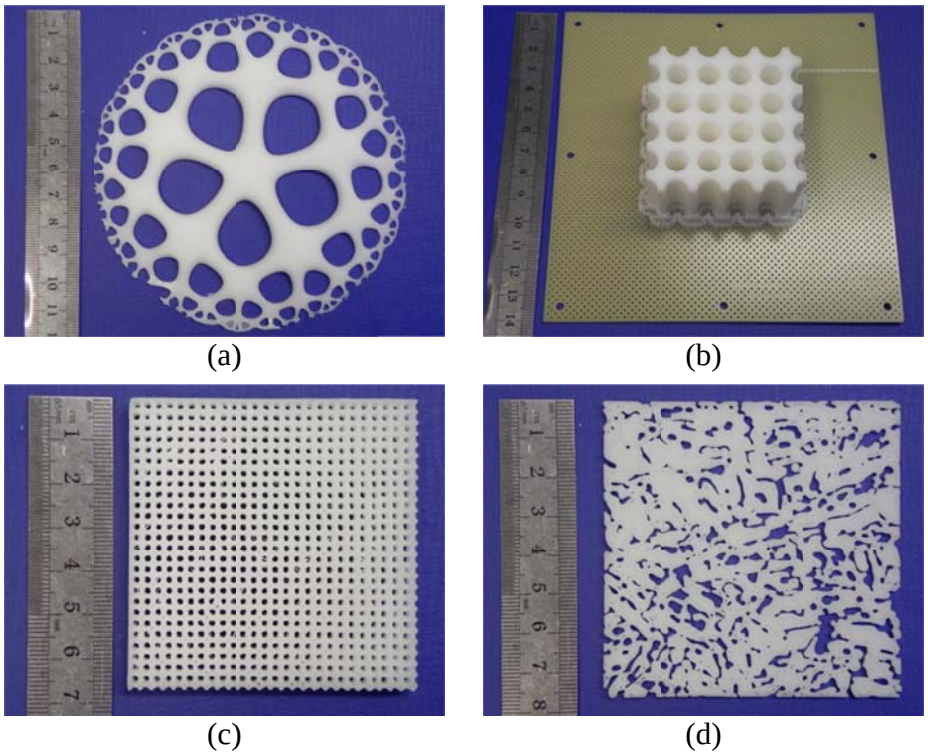

(a) (b)

(c) (d)

Figure 4.3: *Test prints: Echinodermania (Hart (2005)) (a), idealized samples with large round pores (b) and small round pores (c) and a 30 times repeated microtomographic sea-ice image (d).*

After the test prints, sea-ice samples were printed for the permeability experiments in the laboratory. The print models were round in order to fit them into a plexiglass tube with a diameter of 11.4cm. At first, an idealized sample with a given porosity and pore size was created with the module GridGeo in GeoDict. Since only quadratic samples are possible to construct with GeoDict, a circle cutout was made of the constructed sample with Image J. After converting this file with GeoDict into an stl-file, wrong orientated surfaces were repaired and the file size was reduced with Netfabb. The idealized sample had a diameter of 11.2cm and the pore size and porosity were chosen to be 2mm and 0.5%, respectively (Figure 4.4). This pore size is similar to the pore size of a 10 times magnified sea-ice sample. Reducing the distance between pores to gain larger porosities is not possible, because the stl-file becomes too large to be loaded neither in Netfabb nor in the printer program. For unknown reasons the resulting print model (Figure 4.4) had 0.2mm smaller pores than constructed, which resulted in an even smaller porosity of around 0.36%. The print model was planned to have a height of 1cm, but since the role of ABS-filament became empty during printing, the height was only 0.7cm.

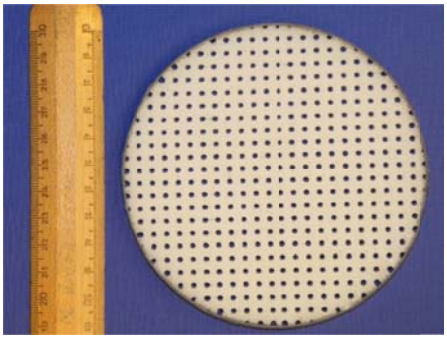

Figure 4.4: *Idealized sea-ice sample.*

Out of the many sea-ice samples three were chosen to be printed. Not all samples can be printed, because it takes some time to print a sample and it is also still expensive. A round sea-ice print model with a diameter of 11.2cm and a height of 1cm costs around 6€ and it takes roughly 12 hours to print the model. Hence, only two first-year ice samples and one laboratory ice sample were printed (Figure 4.5). For printing, the segmented circle cutout of the tomographic image stack was converted into an stl-file with GeoDict and wrong orientated surfaces were repaired and the file size was reduced with Netfabb. Due to the segmentation the solid ice structure is printed as a 3D model. The print models were 10 times magnified compared to the original microtomographic image so that pores of all sizes can be printed. Like the idealized sea-ice print model, the print models of the sea-ice samples had a diameter of 11.2cm in order to fit into a plexiglass tube for the laboratory experiments. The first 100 images of the microtomographic sea-ice image stack were chosen so that the print models had a height of roughly 1cm.
Even though the stl-files of the sea-ice samples were repaired with Netfabb before printing, there still seemed to be some non-repairable parts, because additional material was often printed into the sea-ice pores. This can not be support material, because there were no overhanging parts in the sea-ice pores. Especially in one first-year ice sample (Figure 4.5 (a)) and the laboratory-ice sample (Figure 4.5 (b)) there was too much additional material printed, which was not completely removable from the pores. In the second first-year ice sample (Figure 4.5 (c)) the additional material was less than in the other two samples, which could be removed from the pores (Figure 4.5 (d)). But still in some pores this additional material could not be removed properly, which could impact the results of the permeability experiments. Hence, only the first and the 100th image were taken to create simplified sea-ice samples for the laboratory experiments. Each image was repeated 200 times which resulted in 2.3cm thick print models (Figure 4.6). The height of the simplified sea-ice print models was larger than of the idealized sea-ice print model in order to increase the hydraulic head in the permeability experiments. Inside the pores of these simplified sea-ice samples no additional material was printed. Since the idealized sample already showed that the printed pores are slightly smaller than the original pore sizes, five pores were taken in both simplified samples and compared to the original microtomographic pictures. The result is that the printed pores were around 0.2cm smaller than the original pores of the magnified sea-ice sample. This difference has to be kept in mind for the permeability experiments.

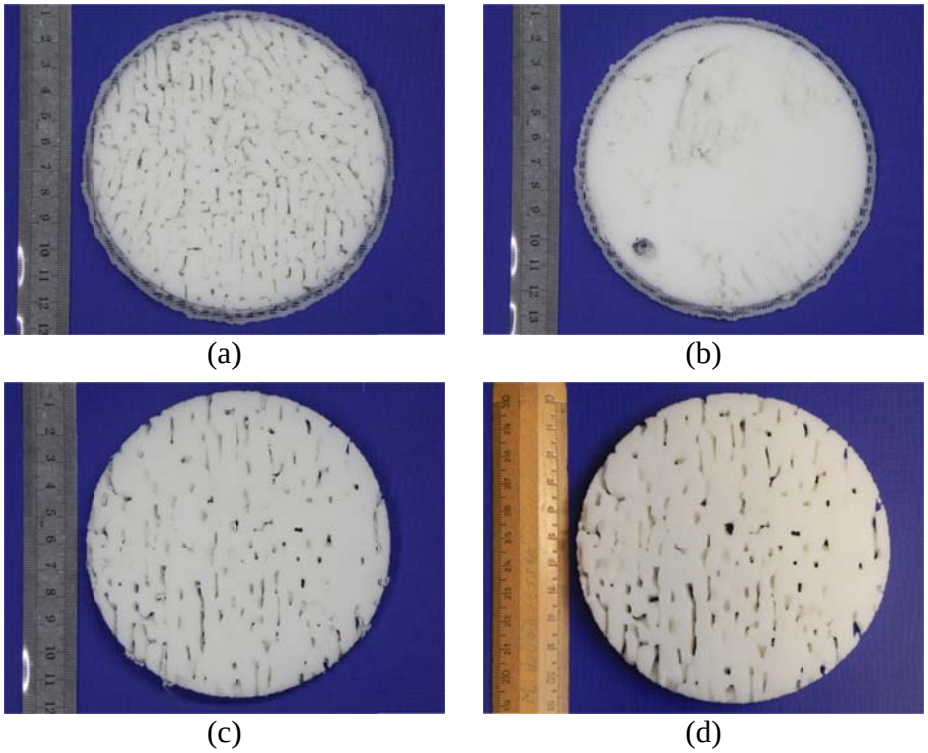

(a) (b)

(c) (d)

Figure 4.5: *Magnified 3D print models of first-year ice (a and c) and laboratory-ice samples (b). In the sea-ice print model shown in (c) the spare material inside the pores was removed (d).*

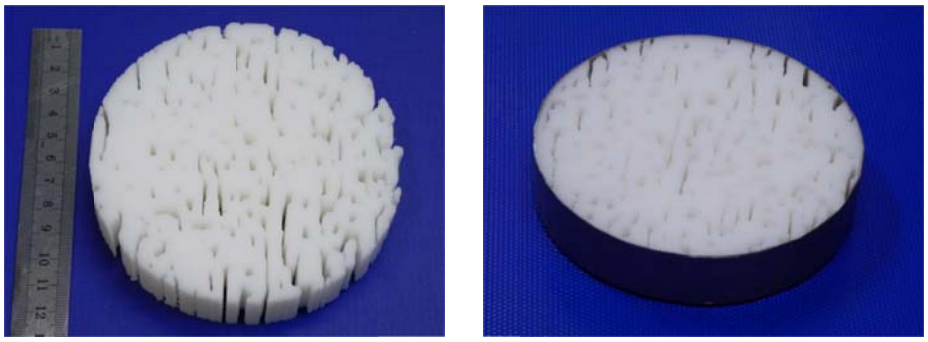

(a) (b)

Figure 4.6: *Simplified 3D sea-ice print models: 200 times repeated image 1 (a) and image 100 (b) of the first-year ice sample shown in Figure 2.1 and 4.5 (c and d).*

5 Laboratory experiments

The concept of the permeability experiments is to let a liquid flow through the 3D print models, similar to the hydrodynamic simulations with GeoDict. Therefore, a liquid is needed that has a high viscosity so that the flow through the pores of the magnified sea-ice print models is laminar. For these experiments canola oil was taken.

The viscosity of the canola oil was determined with a flow cup (Figure 5.1 (a)), which is a simple viscosimeter. The viscosity is calculated out of the time the oil needs to flow through the nozzle of the conical cup. The measurements are conducted as follows: the oil is filled into the cup while the nozzle is closed with a finger. Then, the time is measured from pulling away the finger

from the nozzle (begin of flow) until the flow breaks down. The cup used for these experiments has a volume of 100ml and a nozzle diameter of 4mm. Fritz (1949) conducted several experiments with this flow cup and with different oils at 20°C. He found that for cup efflux times higher than 15s the viscosity of an oil can be calculated from the following empirical equation (Poiseuille equation with Hagenbach correction):

$$\nu = A \cdot t - \frac{B}{t}$$

ν corresponds to the kinematic viscosity in cSt, t to the cup efflux time in s and the two coefficients have the values A = 4.67 and B = 570. In A and B the volume of the cup and the length of the nozzle are comprised amongst others. At cup efflux times less than 15s the influence of the viscosity on the flow decreases and the influence of inertia increases and the viscosity of the fluid has to be calculated differently.
In total, four flow experiments were conducted. They gave a mean cup efflux time of 24.48s, which is above the critical value of 15s. This measured cup efflux time results in a kinematic viscosity of $9.1 \cdot 10^{-5} m^2/s$ and with a density of $920 kg/m^3$ the dynamic viscosity is 0.084Pa·s. According to Przybylski (2001), the viscosity of canola oil is a bit lower at 20°C. A reason for this difference might be that the measurements were conducted at temperatures lower than 20°C. Water has a viscosity of 0.001Pa·s at 20°C, which is nearly 100 times less than the viscosity of canola oil. Hence, canola oil is a suitable fluid for the permeability experiments.

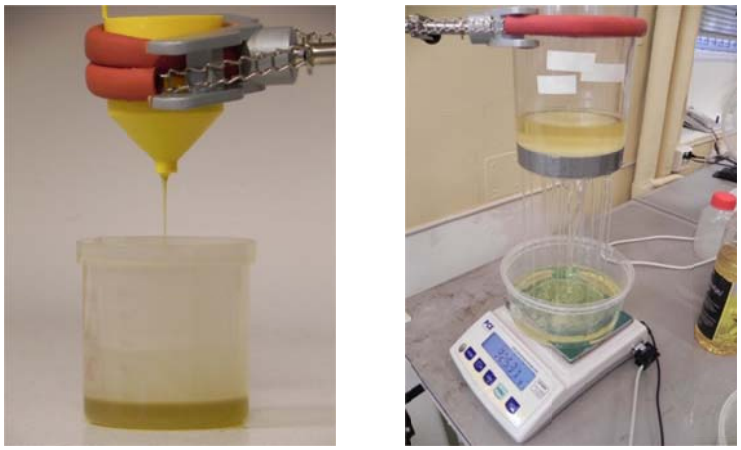

(a) (b)

Figure 5.1: *Measurement of the viscosity of canola oil with a flow cup (a) and a permeability experiment with a simplified sea-ice print model (b).*

The permeability experiments were done with the idealized and the two simplified sea-ice print models (Figure 4.4 and 4.6). Three layers of duct tape where put around each sample (Figure 4.6 (b)). Like this, the print models could be placed tightly at one end of a pelxiglas tube, into which the oil was filled in order to flow through the print model (Figure 5.1 (b)). To prevent the oil from flowing already through the sea-ice print model out of the tube while filling the oil into the tube, a plastic lid was held underneath the print model. A 4.8mm thick and 9.5mm wide stripe of Neopren rubber was glued with hot glue in a circle onto the plastic lid for sealing. Nevertheless, at an oil height of more than 7cm, the oil could not be completely held back with this technique

and some oil started flowing out of the tube. A plastic box was placed on scales underneath the tube. By measuring the weight every second the change in oil height above the print model can be calculated during the flow. Before letting the oil flow through the print model by pulling away the plastic lid, the oil height above the print model was marked with a little piece of tape on the tube. With these measurements the permeability of the print models could be calculated from Darcy's law.
Due to lack of time only few experiments were performed. During the experiments some problems occurred so that there are no results to be shown yet. In the experiment with the idealized sample the oil was flowing too fast through the print model (within two to three seconds) so that a detailed measurement of the weight difference was not possible. Therefore, the two simplified sea-ice print models were printed more than twice as thick as the idealized sea-ice print model and a bit more oil was filled into the tube. But still there occurred some problems during the measurements. Sometimes the oil started already flowing out of the tube before the begin of an experiment. Additionally, some oil was lost on the table around the scales by pulling away the lid. Hence, the oil height was differently between experiments and had to be marked newly in each experiment. Marking the oil height was not easy on the oily plexiglas tube while holding the lid underneath the sea-ice print model, which gives inaccurate values. Another technique for holding the oil back during filling the oil into the tube should be invented.

Bibliography

Fritz, W. (1949). Bemerkungen zum Auslaufbecher din 53211. *Chemie Ingenieur Technik*, 21(5-6):103–105.

Hart, G. W. (2003-2005). http://www.georgehart.com/rp/rp.html.

Przybylski, R. (2001). Canola oil: physical and chemical properties. *Canola council of Canada*, 1.

Wiegmann, A. (2012). Geodict, Fraunhofer Institut für Techno-und Wirtschaftsmathematik.